Ultrafast carrier dynamic anisotropy of single crystal rhenium disulfide flake based on transient absorption spectroscopy

Xiaodan Zhang, a,b Lihe Yan, a,b,* Yanmin Xu, a,b Jinhai Si,a,b and Xun Houa,b aXi'an Jiaotong University, School of Electronics Science and Engineering, Key Laboratory for Physical Electronics and Devices of the Ministry of Education, Xi'an, China bShaanxi Key Lab of Photonic Technique for Information, Faculty of Electronic and Information Engineering, Xi'an, China

Abstract. In recent years, rhenium disulfide (ReS₂) has attracted much attention in polarization dependent photonic applications due to its anisotropic optoelectronic response. To reveal the anisotropic response mechanisms, single crystal layered ReS₂ flake with lateral size of about $10 \mu m$ is obtained using mechanical exfoliation method, and the ultrafast carrier dynamics of an individual flake is studied using transient absorption microscopy. The excited carrier concentration of layered ReS₂ flake exhibits obvious polarization dependence of the pump light, which is caused by the anisotropic linear absorption and electron mobility rates in different orientations. These results could provide more references for the application of ReS₂ in polarization sensitive detectors and optoelectronic devices. © 2023 Society of Photo-Optical Instrumentation Engineers (SPIE) [DOI: 10.1117/1.OE.62.4.047102]

Keywords: ultrafast carrier dynamics; layered rhenium disulfide flake; femtosecond time-resolved transient absorption microscopy.

Paper 20230047G received Jan. 16, 2023; revised manuscript received Mar. 19, 2023; accepted for publication Apr. 6, 2023; published online Apr. 22, 2023.

1 Introduction

Since the discovery of graphene in 2004, the exploration and applications of two-dimensional (2D) materials have attracted much attention.¹ For 2D materials, including black phosphorus (BP),²⁻⁴ topological insulator,⁵ transition metal dichalcogenide,⁶⁻⁸ etc., the atoms within the layers are connected by strong covalent bonds, and the layers are bonded by van der Waals forces. Due to their unique structures, 2D materials have made great progress in optoelectronic devices, such as transistors, photodetectors, all-optical switches.⁹⁻¹¹ For van der Waals materials, they have the strong out-of-plane anisotropic structure, leading to the large intrinsic birefringence and low loss, and are considered as candidates for next-generation photonics.¹² Recently, different kinds of in-plane isotropic materials with symmetrical lattice structures, such as MoS₂ and graphene materials, have exhibited excellent optical and electrical properties and have been used in transistors, saturable absorbers and so on.

In 2014, Wang et al.¹³ used BP in field effect transistors (FETs) for the first time, and then anisotropic 2D materials came into the insight. To be different from graphene and MoS₂, in such anisotropic 2D materials as BP, tin selenide (SnSe), ^{14,15} rhenium disulfide (ReS₂), ^{16,17} the periodicity and sparsity of atom arrangements on the plane differ a lot with the directions of the lattice. Usually, armchair and zigzag directions are used to characterize the different axis in the 2D nanosheets layer plane, while the material shows different carrier mobility between the armchair and zigzag directions. ^{18–20} Due to their special lattice structure, the optical and electrical properties of anisotropic materials exhibit a strong dependence on the crystal orientation, which makes them good candidates for the fabrication of polarization dependent optoelectronic devices. ^{21,22} Among these anisotropic 2D materials, ReS₂ possesses a distorted 1T phase structure, while the weak interlayer coupling allows a direct bandgap independent of the thickness, as well as

0091-3286/2023/\$28.00 © 2023 SPIE

-

^{*}Address all correspondence to Lihe Yan, liheyan@mail.xjtu.edu.cn

wide applications in optoelectronics.²³ For example, Zhang et al.²⁴ studied the electrical properties of ReS₂-based FET and found that conductivity measured parallel and vertical to the Re-Re axis (zigzag direction) reached the maximum and minimum, respectively. Recently, Meng et al.²³ demonstrated the anisotropy of optical nonlinearity in ReS₂, which exhibited a transition from saturation absorption to anti-saturation absorption by varying the incident light polarization. In addition, there are several reports demonstrating the anisotropy of the out-of-plane optics of ReS₂ and ReSe₂,^{25,26} providing a theoretical basis for the application of all-dielectric nanophotonics. Anton A et al.²⁷ calculated the dielectric constant variation under different polarized light via time-dependent density functional theory and demonstrated the significant biaxial anisotropy attributed to in-plane structures with low symmetry.

The generation and transport characteristics of photoinduced carriers affect the optoelectronic properties in ReS₂ greatly, and clarifying the anisotropic ultrafast dynamics of photogenerated carriers is of great significance for deeply understanding the optoelectronic response and mechanisms. Femtosecond time-resolved transient absorption (fs-TA) spectroscopy has been demonstrated to be a powerful method to study the photo-induced carrier kinetics in materials. However, the application of fs-TA technique in anisotropic 2D materials has been rarely reported. As the 2D nanosheets prepared by chemical vapor deposition method often show weak anisotropic property, mechanical exfoliation is usually used to prepare samples with good monocrystalline feature. Because the size of the sample made by mechanical exfoliations is quite small and the probing area of conventional fs-TA technology is large (\sim 10 μ m), the carrier behavior in an individual nanosheet cannot be accurately obtained. Thereby, fs-TA microscopy (fs-TAM) techniques with high spatial resolution are needed to study the carrier dynamics of single crystal samples.

In this paper, we studied the anisotropy of photogenerated carrier dynamics in layered ReS_2 flakes by fs-TAM spectroscopy. ReS_2 flake was prepared by mechanical exfoliation, and the photogenerated carrier dynamics of single crystal ReS_2 flakes was analyzed. The relaxation process of the carrier of the single crystal ReS_2 flakes showed the two lifetimes of 0.6 ps and \sim 2.1 ns, which corresponds to the formation of hot carriers and formation of excitons, respectively. By changing the polarization angle of the pump light, the carrier concentration shows obvious anisotropy, which was attributed to the anisotropic linear absorption and electron mobility rates in different orientations. As a comparison, convention TA measurements were performed with several flakes with different orientations excited simultaneously, and the carrier concentration showed independence on the pump polarization.

2 Experimental Section

The single crystal ReS₂ flakes studied in this paper were prepared by mechanical exfoliation method. By overcoming the van der Waals force between the layers of bulk ReS₂ through the adhesive force of the tape, 2D flakes materials can be obtained. The morphology and chemical structure of the peeled flakes were then characterized by the methods described in Sec. 2.2.

2.1 Preparation of Flakes

The bulk ReS₂ material was purchased from SixCarbon Technology ShenZhen (the purity >99.999%), and the 3M tape was purchased from XFNano Materials Tech Co, Ltd. (Nanjing, China). At room temperature, a piece of smooth ReS₂ material was placed on 3M tape and repeatedly glued to clean tape until the residual color was almost transparent. The side with the ReS₂ sample was then glued to the treated quartz substrate and gently pressed with a cotton swab to make them fully bonded. After 2 hrs, the ReS₂ flakes were successfully stripped and then stored in the airtight box for further testing.

2.2 Characterization

Atomic force microscopy (AFM, Bruker) was used to measure the thickness and topography of flakes. The crystallization properties of the flakes were analyzed by the x-ray diffractometer (XRD, Bruker). The absorption spectrum was detected by ultraviolet and visible (UV)

spectrophotometer. Due to the small size of the exfoliated flakes and the lower accuracy of spectrophotometer, layered ReS₂ flake showed very weak absorption. To measure the absorption of the material accurately, absorption spectra of multiple ReS₂ flakes on the substrate was measured, and the measurement range of the spectrum is 200 to 1400 nm. For the polarization Raman spectroscopy (Renishaw), the low-power nanosecond laser (excitation wavelength of 532 nm) is used as the excitation light source, and the test system has a microscopic imaging function. The photoluminescence (PL) spectra of flakes were also performed using this system. All of the samples tested above were prepared by mechanical exfoliation and peeled onto the quartz substrate.

2.3 Femtosecond Time-Resolved Transient Absorption Microscopy

The laser source was a Ti: sapphire mode-locked fs laser (Coherent, United States) emitting pulses with the pulse width of 65 fs, center wavelength of 800 nm, and repetition frequency of 1 kHz. The output of the laser was divided into two beams: the stronger one was frequency doubled and used as the pump light, and the weaker one was focused into a sapphire plate generating supercontinuum probe light ranging from 450 to 950 nm. The pump light and the probe light were focused on the sample through a home-built microscopic imaging unit with a $20\times$ objective lens. The laser passing through the sample was collimated and the pump light was filtered using a long-pass filter with a cut-off wavelength of 450 nm. In the experiment, the difference between the arrival time of the pump and the probe pulses to the sample was varied by motorized displacement stage, and finally the probe pulse passing through the sample was collected by fiber-coupled spectrometer. After the sample was excited, the optical density change (Δ OD) of the probe light as a function of the delay time between the pump and probe pulses can be obtained by comparing the absorption of the probe light with (Δ OD) and without (Δ OD) pump light excitation

$$\Delta \text{OD}(\lambda, t) = \text{OD}_{\text{pump}} - \text{OD}_{\text{umpump}} = \log \frac{I_0}{I_{\text{pump}}} - \log \frac{I_0}{I_{\text{umpump}}} = \log \frac{I_{\text{umpump}}}{I_{\text{pump}}}, \quad (1)$$

where λ is the wavelength of the probe light, t is the delay time representing the time delay of the pump pulse to the probe pulse, I_0 is the intensity of the incident probe light, and I_{pump} and I_{umpump} are the probe pulse intensity passing through the sample with and without pump light excitation. All the experiments in this work were performed at room temperature (295 K).

3 Experimental Results and Discussions

The ReS₂ flakes were successfully prepared by mechanical exfoliation with scotch tape from the bulk crystal, and the specific operation process is shown in Sec. 2.1. In the preparation of 2D materials, the size and thickness of the material are of great importance. Figure 1(a) shows the typical AFM image of the exfoliated layered ReS2 flake. It is noted that the red dashed circle marks the irradiation area of pump pulse in fs-TAM measurements. As shown in the figure, the ReS₂ flake is distributed on the quartz substrate and the surface of the sample is relatively uniform. The size is measured to be about $10 \times 15 \ \mu \text{m}^2$. In ReS₂, due to the stronger bond energy along the Re-Re metal atom chain, the crystal preferentially breaks in this linear direction. 30,31 The crystal axis of ReS₂ which is defined as the zigzag axis can be roughly determined by the long cleaved edge, while the direction perpendicular to the Re chain is usually noted as the armchair direction. Figure 1(b) is the cross-sectional height view of the flake as indicated by the solid white line in Fig. 1(a), showing the thickness of 37 nm. XRD characterization is used to detect the crystallization of the flakes [Fig. 1(c)]. XRD patterns of ReS₂ flakes show diffraction peaks of (100), (002), (02-1), (201), (003), (20-3), (022), and (004), which are consistent with the standard powder diffraction file (PDF) card (00-052-0818). The four main diffraction peaks show sharp shapes, and there are few miscellaneous peaks nearby. The results indicate that the nanomaterials prepared by mechanical exfoliation possess a high degree of crystallization.

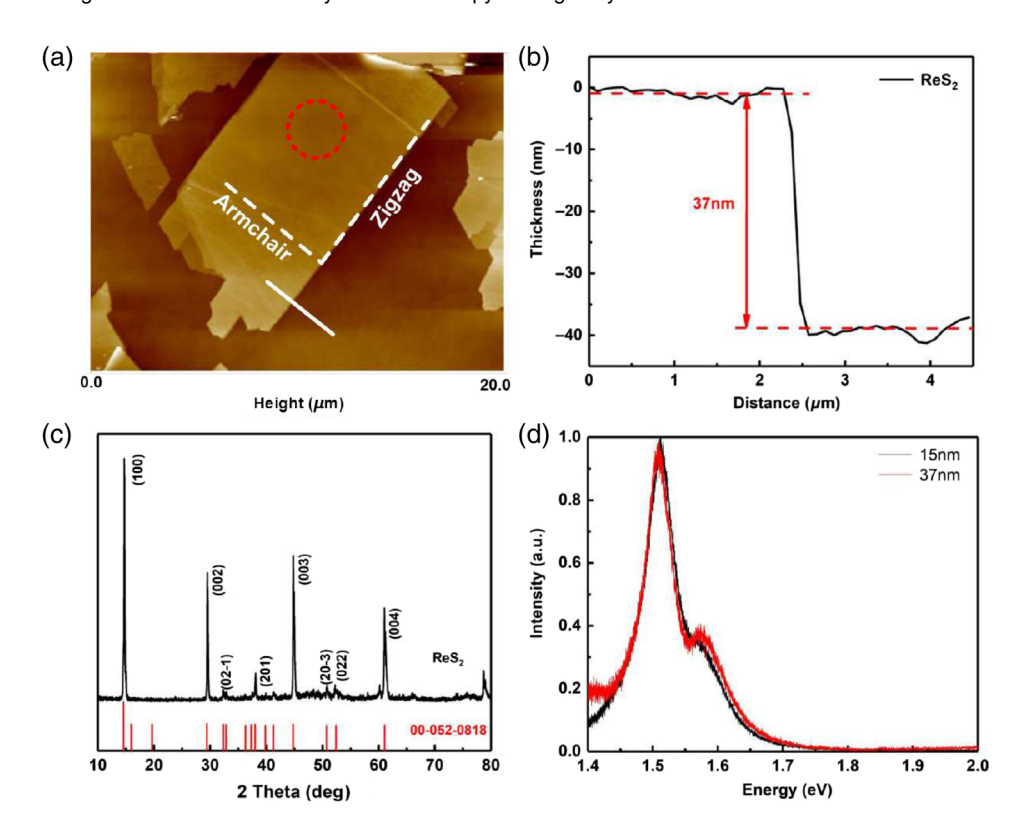


Fig. 1 (a) AFM image of single crystal ReS_2 flake. The red dashed circle indicates the pump light irradiation area in the fs-TAM measurements. (b) The height profiles of ReS_2 along the solid white line are indicated in (a). (c) XRD patterns of ReS_2 and the PDF card of ReS_2 are shown in red. (d) Normalization PL spectra of ReS_2 with different thicknesses at room temperature.

The PL properties of ReS₂ flakes are analyzed using PL spectroscopy. The normalized PL spectra of ReS₂ with thickness of about 15 and 37 nm are shown in Fig. 1(d). The single crystal ReS₂ flake has two exciton peaks, with the lower energy peak at about 1.51 eV, and the higher located at 1.57 eV. The lower energy peak originates from the polarized emission of electronhole pairs (excitons) along the Re-Re chain, and the higher energy peak originates from electronhole pairs along the Re-S chain.³² The polarization emission of the two different excitons may be related to the low symmetry and anisotropic dielectric shielding effect in ReS₂.⁷ With the sample thickness increased, the polarization emission position of the characteristic excitons does not change, indicating that ReS₂ has weak interlaminar coupling and maintains the electronic structure of the direct bandgap.

As shown in Fig. 2(a), the ReS₂ flakes exhibit an absorption peak at around 610 nm, which can be attributed to the interband excitonic transition at the K point of the Brillouin zone.³³ According to the Kubelka-Munk formula, the bandgap of ReS₂ flakes is estimated to be 1.50 to 1.6 eV, according to some previous reports.³⁴ To analyze the structure of the crystal, polarized Raman spectroscopy is performed on the flakes as shown in Fig. 2(b). In ReS₂, the Re atoms and the S atoms are in the same plane, and this causes anisotropic lattice vibrations in and out of the plane.³⁵ As shown by the figure, the spectrum displays more than 18 vibration modes in the range of 100 to 500 cm⁻¹, with six featured modes in the range of 100 – 240 cm⁻¹ (denoted as Mode I to VI).³⁶ Among them, vibration modes I and II located at 136.8 and 144.5 cm⁻¹ correspond to the out-of-plane vibration of Re atoms, while the modes III to VI located at 153.6, 163.4, 212.4, and 238.1 cm⁻¹ correspond to the in-plane vibration of Re atoms. The results are consistent with the Raman spectra reported in the previous studies.³⁷ With the change of polarization angle, the peak intensity is significantly different, but the position of the characteristic peak is basically unchanged.

To quantitatively study the Raman spectra, the peak intensity of Mode V as a function of the angle between the laser polarization and the long cleaved edge is measured, and the results are

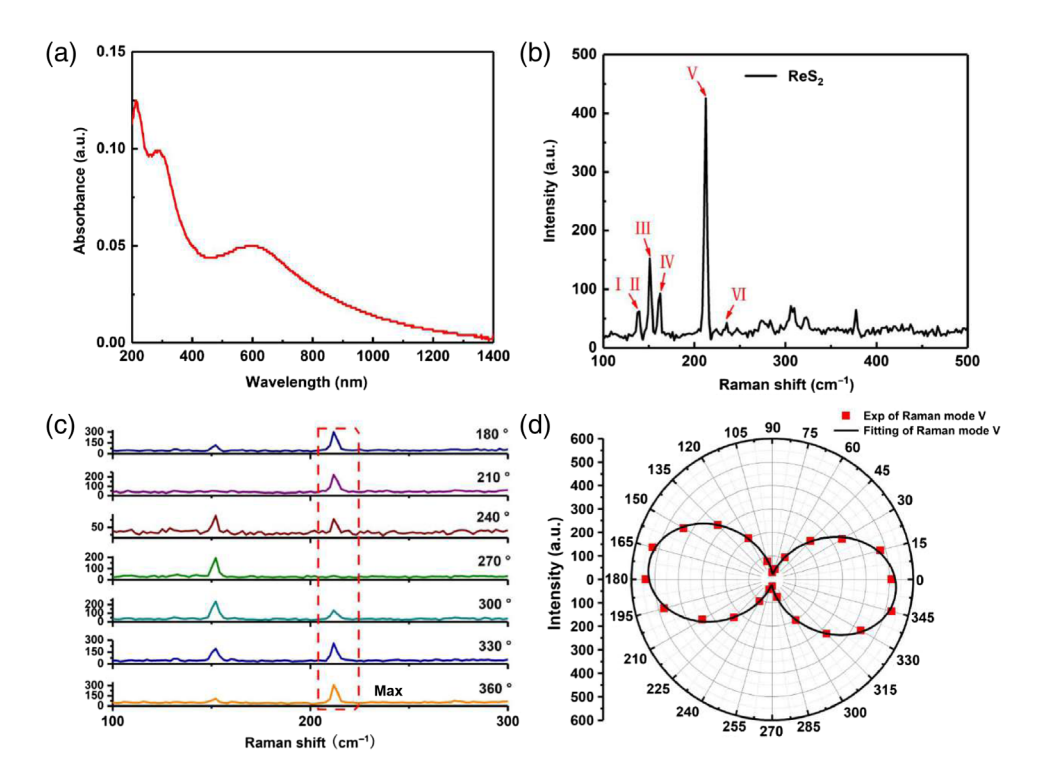


Fig. 2 The optical characterizations of ReS_2 . (a) UV-vis absorption spectra. (b) Raman spectrum of the ReS_2 flakes. (c) The Raman spectra of single crystal ReS_2 flakes at different polarization angles (180 deg to 360 deg). The red dashed box indicates the intensity change of Mode V. (d) The polar plots of Mode V spectral intensity as a function of the polarization angle. The red squares are the experimental data points, and the solid black lines are the fitted curves using Eq. (2).

given in Fig. 2(c). Figure 2(d) summarizes the polarization-dependent Raman intensity, which can be well fitted using the equation:

$$I = a + b\cos^2(\theta - \theta_{\text{max}}),\tag{2}$$

where a and b are constants, I represents the Raman intensity, θ is the angle between the laser polarization and the long cleaved edge, and θ_{max} represents the angle corresponding to the maximum value of intensity. Besides, the value of a+b corresponds to the maximum value of the signal intensity, while a represents the minimum value of the intensity, and the anisotropy ratio can be calculated by the formula as $1+\frac{b}{a}$. The intensity of Mode V reaches the maximum when the incident light is parallel to the long cleaved edge (0 deg and 180 deg), and has the lowest intensity when the directions are perpendicular (90 deg and 270 deg). According to the previous studies, 38 the direction corresponding to the maximum intensity of Mode V is the zigzag axis of ReS₂, which is in accordance with the long cleaved edge direction in Fig. 1(a).

To study the photoinduced carrier dynamics of 2D materials, we provide a TA test system with microscopic function, and the detailed settings are shown in the experiment section above. In the experiments, the pump and probe beams are focused into the sample using an objective lens and the diameter of the incident laser spot is about 2 μ m, which is much smaller than the lateral size of sample. The irradiation area of pump light is indicated by the red circle in Fig. 1(a). Figure 3 shows the dependence of carrier behavior of ReS₂ flakes on polarization, which was obtained by the fs-TAM technique. Figure 3(a) shows the TA spectra of sample at different time delays. Around 800 nm, the spectrum displays the significant negative signal, and the signal intensity tends to decrease with time delay. This signal may come from the ground state bleaching effect of excitons along the Re-Re crystal axis³⁹ [corresponding to the zigzag axis in Fig. 1(a)]. Generally, electrons in the material can absorb white probe light, inducing a strong exciton absorption signal. When pump light irradiates the sample, excitons are excited and dissociate into excited electrons and holes. The excited electrons and holes could fill in the

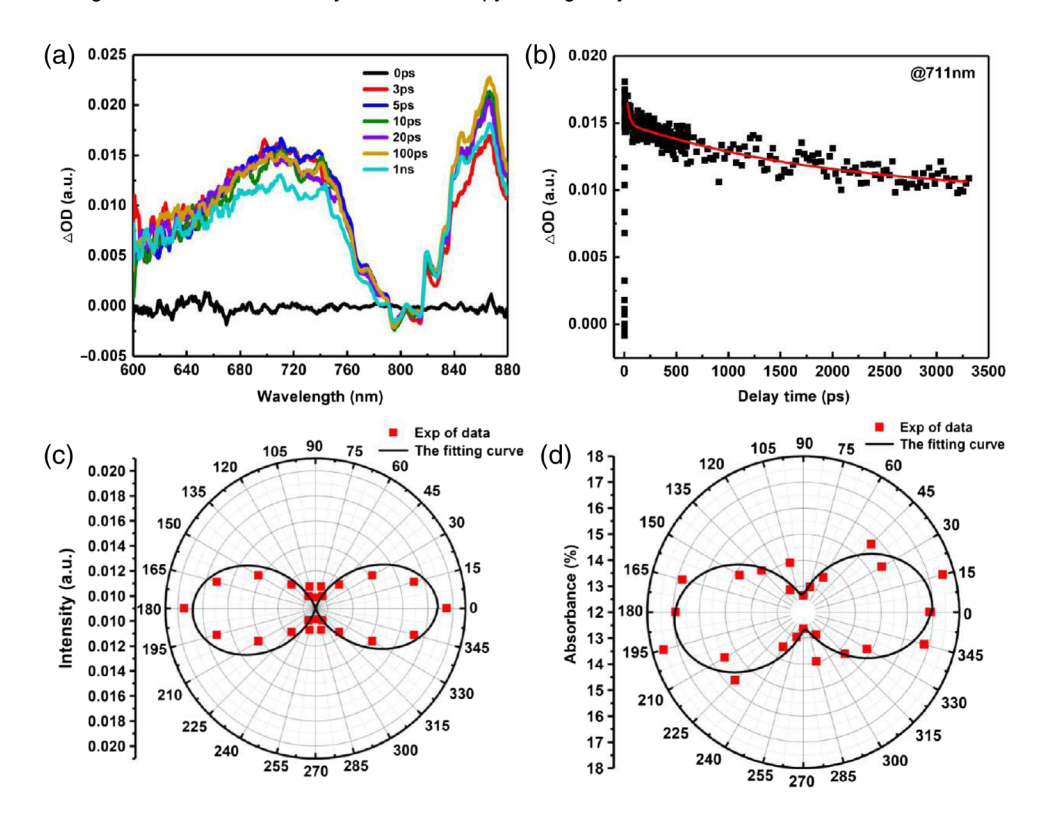


Fig. 3 (a) Fs-TAM spectra with different delay times with the pump wavelength of 400 nm. (b) Carrier dynamics process of ReS_2 flakes with the probe wavelength of 711 nm. (c) The TA spectra peak of ReS_2 at different laser polarization angles. (d) The linear absorptance versus polarization angle with respect to the zigzag axis in polar coordinates. The red squares are the experimental data points, and the solid black lines are the fitted curves using Eq. (2) in panels (c) and (d).

conduction band and valance band respectively, reducing the absorption of probe light, namely ground state bleaching effect. Besides, the spectra show clear excitation state absorption signals at 711 and 860 nm. With the increase of the delay time, the absorbance signal gradually decreases synchronously with the ground state bleaching signal. To reveal the decay process of the ground state bleaching and excitation state absorption, the decay signals of the probe light at wavelength of 711 nm was well fitted using the double exponential function, as shown in Fig. 3(b). The two time constants, $\tau_1 = 0.6$ ps and $\tau_2 = 2.1$ ns, were obtained. The slow time constant τ_2 is attributed to the relaxation of hot carriers and the formation of excitons, and the fast time constant τ_1 corresponds to the formation of hot carriers and establishes the quasi-equilibrium Fermi distribution.⁴⁰

Based on the unique lattice structure of ReS_2 , the effect of anisotropic properties on carrier dynamics of single crystal ReS_2 flakes is studied by changing the polarization angle of pump light. The polarization direction of the laser is set as 0 deg when it is parallel to the zigzag axis of the flakes, and 90 deg when perpendicular. In Figs. 3(c) and 3(d), both TA signal intensity and linear absorption were fitted using the same equation as the Raman intensity of Mode V. As shown in Fig. 3(c), excited state absorption signal intensity at the same delay time changes periodically with the polarization angle. Here, the delay time was fixed at 5 ps, when the excited state absorption signal at 711 nm reached the maximum. The peak value of the TA reaches the maximum when the polarization angle is parallel to the long cleaved edge (0 deg, 180 deg), and minimum when the polarization is perpendicular (90 deg, 270 deg). To clarify the origin of the anisotropic carrier dynamics in the flakes, we measure the polarization dependence of the absorption of pump light using the fs-TAM system. The incident laser power is fixed at 30 μ W, avoiding the occurrence of nonlinear optical effects. As shown in Fig. 3(d), the linear absorption also shows a slight anisotropy with the polarization angle of the pump light, with the

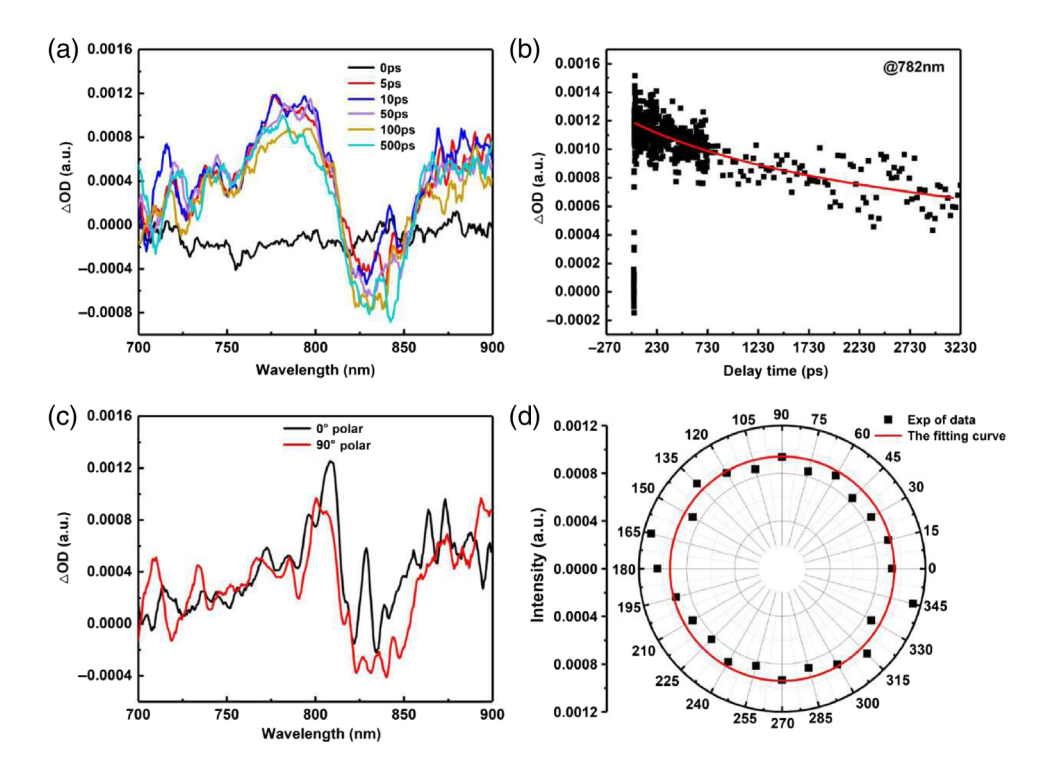


Fig. 4 (a) Fs-TA spectra with different delay times with the pump wavelength of 400 nm. (b) Carrier dynamics process of ReS₂ flakes with the probe wavelength of 782 nm. (c) The comparison of TA spectra of ReS₂ flakes at different polarization angles. (d) The TA spectra peak of ReS₂ at different laser polarization angles.

maximum and minimum taking place at 0 deg and 90 deg, respectively. The different linear absorption could cause the variation of excitation probability of the electrons, causing the anisotropy of carrier dynamics. This result is in accordance with the findings reported by Ho et al.,³⁹ in which the anisotropic response was attributed to the different reflectance by ReSe₂. However, when carefully comparing the anisotropy of the carrier dynamics and linear absorption, we find that the anisotropy ratio of the excited carrier density is estimated to be about 1.9, being much larger than that of the linear absorption with the ratio of 1.35. This indicates that, besides the linear absorption anisotropy, some other effects could also contribute to the anisotropic carrier dynamics. Yu et al.¹⁷ have reported that both electron and hole mobilities of ReS₂ were highly anisotropic, with a maximum electron mobility along the b-axis of about 799.64 cm²/Vs. Thereby, we attribute the large excited state carrier concentration along the zigzag axis to the combined effect of the maximum electron mobility rate and the maximum linear absorption.

To further confirm the carrier anisotropy characteristics in layered ReS₂ flakes, the carrier dynamics of the sample is studied using conventional TA spectroscopy. In the conventional TA measurements, the size of the pump light spots is about $100~\mu m$, and there are several ReS₂ flakes distributing randomly and excited simultaneously in the pump light irradiation area. Figure 4(a) shows the TA spectrum with a significant negative signal at 830 nm, which is also related to the ground state bleaching effect of excitons along the Re-Re crystal axis. Figure 4(b) shows the carrier relaxation process of the ReS₂ flakes, which can be fitted using a double-exponential function with the time constants of 1.2 and 12.4 ns. The peak position and decay process of the ground state bleaching signal are slightly different from the results obtained in an individual ReS₂ flake, which could be mainly due to the ensemble average effect of the different size, orientation and thickness of different flakes. Also because of this reason, the TA spectra changes little with changing the polarization angle of the pump light, as shown in Figs. 4(c) and 4(d). By comparing the polarization dependence of the TA signals obtained using TAM and conventional TA measurements, the anisotropic response of the carrier dynamics in single crystal ReS₂ flake is further confirmed.

4 Conclusion

In summary, we studied the photogenerated carrier dynamics of the single crystal ReS₂ flakes using the fs-TAM spectroscopy. The samples were successfully prepared by mechanical exfoliation, and the ultrafast carrier dynamics process was further analyzed. When the sample is irradiated with the fs pulse, the photogenerated carriers showed the two distinct relaxation processes (0.6 ps and 2.1 ns), corresponding to the formation and relaxation of hot carriers, respectively. Besides, due to the combined effect of linear absorption and electron mobility rates anisotropy in single crystal ReS₂ flakes, we found that the peak values of the TA spectrum exhibit anisotropy in relation to the crystal axis with changing the polarization angle of the pump light. The experimental results in this paper revealed the polarization-dependent characteristics of carriers in single crystal ReS₂ flakes, which provide a nonlinear theoretical basis for applications in polarization detectors and optical switches.

Acknowledgments

This work is supported by the National R&D Program of China (Grant No. 2019YFA0706402) and the National Natural Science Foundation of China (Grant No. 62027822). The authors declare no conflicts of interest.

References

- 1. K. S. Novoselov et al., "Electric field effect in atomically thin carbon films," *Science* **306**(5696), 666–669 (2004).
- 2. X. Liang et al., "Photothermal cancer immunotherapy by erythrocyte membrane-coated black phosphorus formulation," *J. Control Release* **296**,150–161 (2019).
- 3. H. Liu et al., "Black phosphorus-film with drop-casting method for high-energy pulse generation from Q-switched Er-doped fiber laser," *Photonic Sens.* **9**(3), 239–245 (2019).
- 4. Y. H. Wang et al., "Ultrafast recovery time and broadband saturable absorption properties of black phosphorus suspension," *Appl. Phys. Lett.* **107**(9), 091905 (2015).
- 5. Y. Chen et al., "The formation of various multi-soliton patterns and noise-like pulse in a fiber laser passively mode-locked by a topological insulator based saturable absorber," *Laser Phys. Lett.* **11**(5), 055101 (2014).
- 6. Y. Xu et al., "Nonlinear absorption properties and carrier dynamics in MoS2/graphene van der Waals heterostructures," *Carbon* **165**, 421–427 (2020).
- 7. H. Zhao et al., "Interlayer interactions in anisotropic atomically thin rhenium diselenide," *Nano Res.* **8**(11), 3651–3661 (2015).
- 8. Y. Zhou et al., "Stacking-order-driven optical properties and carrier dynamics in ReS₂," *Adv. Mater.* **32**(22), 1908311 (2020).
- F. Liu et al., "Highly sensitive detection of polarized light using anisotropic 2D ReS₂," Adv. Funct. Mater. 26(8), 1169–1177 (2016).
- 10. Q. H. Wang et al., "Electronics and optoelectronics of two-dimensional transition metal dichalcogenides," *Nat. Nanotechnol.* **7**(11), 699–712 (2012).
- 11. C. Zhang et al., "Anisotropic nonlinear optical properties of a snse flake and a novel perspective for the application of all-optical switching," *Adv. Opt. Mater.* **7**(18), 1900631 (2019).
- 12. G. A. Ermolaev et al., "Giant optical anisotropy in transition metal dichalcogenides for next-generation photonics," *Nat. Commun.* **12**(1), 854 (2021).
- 13. F. Xia, H. Wang, and Y. Jia, "Rediscovering black phosphorus as an anisotropic layered material for optoelectronics and electronics," *Nat. Commun.* 5, 4458 (2014).
- T. Yan et al., "Ultrafast carrier relaxation in SnSex (x=1, 2) thin films observed using femtosecond time-resolved transient absorption spectroscopy," *Opt. Mater.* 108, 110440 (2020).
- 15. S. Yang et al., "Highly-anisotropic optical and electrical properties in layered SnSe," *Nano Res.* **11**(1), 554–564 (2017).

- Y. Xiong et al., "Electronic and optoelectronic applications based on ReS₂," *Phys. Status Solidi Rapid Res. Lett.* 13(6), 1800658 (2019).
- 17. S. Yu et al., "Strain-engineering the anisotropic electrical conductance in ReS₂ monolayer," *Appl. Phys. Lett.* **108**(19), 191901 (2016).
- 18. X. Wang et al., "Highly anisotropic and robust excitons in monolayer black phosphorus," *Nat. Nanotechnol.* **10**(6), 517–521 (2015).
- 19. C. H. Ho et al., "Optical absorption of ReS₂ and ReSe₂ single crystals," *J. Appl. Phys.* **81**(9), 6380–6383 (1997).
- S. Das, M. Demarteau, and A. Roelofs, "Ambipolar phosphorene field effect transistor," ACS Nano 8, 11730–11738 (2014).
- 21. H. Liu et al., "Nonlinear optical properties of anisotropic two-dimensional layered materials for ultrafast photonics," *Nanophotonics* **9**(7), 1651–1673 (2020).
- 22. Z. Zhou et al., "Optical and electrical properties of two-dimensional anisotropic materials," *J. Semicond.* **40**(6), 061001 (2019).
- 23. X. Meng et al., "Anisotropic saturable and excited-state absorption in bulk ReS₂," *Adv. Opt. Mater.* **6**(14), 1800137 (2018).
- 24. E. Zhang et al., "Tunable ambipolar polarization-sensitive photodetectors based on high-anisotropy ReSe₂ nanosheets," *ACS Nano* **10**(8), 8067–8077 (2016).
- 25. A. Mikhin et al., "Bulk ReSe₂: record high refractive index and biaxially anisotropic material for all-dielectric nanophotonics," Mesoscale and Nanoscale Physics (2023).
- 26. F. Mooshammer et al., "In-plane anisotropy in biaxial ReS₂ crystals probed by nano-optical imaging of waveguide modes," *ACS Photonics* **9**(2), 443–451 (2022).
- 27. S. Anton et al., "High refractive index and extreme biaxial optical anisotropy of rhenium diselenide for applications in all-dielectric nanophotonics," *Nanophotonics* **9**(16), 4737–4742 (2020).
- 28. T. Huo et al., "Ultrafast photoinduced carrier dynamics in single crystalline perovskite films," *J. Mater. Chem. C* **11**(11), 3736–3742 (2023).
- 29. C. Wang et al., "Strongly luminescent and highly stable CsPbBr₃/Cs₄PbBr₆ core/shell nanocrystals and their ultrafast carrier dynamics," *J. Alloys Compd.* **946**, 169272 (2023).
- 30. E. Liu et al., "Integrated digital inverters based on two-dimensional anisotropic ReS₂ field-effect transistors," *Nat. Commun.* **6**, 6991 (2015).
- 31. L. Huang et al., "Anomalous fracture in two-dimensional rhenium disulfide," *Sci. Adv.* **6**(47), eabc2282 (2020).
- 32. B. Aslan et al., "Linearly polarized excitons in single- and few-layer ReS₂ crystals," *ACS Photonics* **3**(1), 96–101 (2015).
- 33. S. Liu et al., "Nonlinear optical properties of few-layer rhenium disulfide nanosheets and their passively Q-switched laser application," *Phys. Status Solidi-a* **216**(7), 1800837 (2019).
- 34. T. K. Pathak, H. C. Swart, and R. E. Kroon, "Structural and plasmonic properties of noble metal doped ZnO nanomaterials," *Phys. B Condens. Matter* **535**, 114–118 (2018).
- 35. X. Wang et al., "Direct and indirect exciton dynamics in few-layered ReS₂ revealed by photoluminescence and pump-probe spectroscopy," *Adv. Funct. Mater.* **29**(6), 1806169 (2018).
- A. McCreary et al., "Intricate resonant Raman response in anisotropic ReS₂," *Nano Lett.* 17(10), 5897–5907 (2017).
- 37. D. A. Chenet et al., "In-plane anisotropy in mono- and few-layer ReS₂ probed by Raman spectroscopy and scanning transmission electron microscopy," *Nano Lett.* **15**(9), 5667–5672 (2015).
- 38. X. He et al., "Chemical vapor deposition of high-quality and atomically layered ReS₂," *Small* **11**(40), 5423–5429 (2015).
- 39. J. Z. He et al., "Ultrafast transient absorption measurements of photocarrier dynamics in monolayer and bulk ReSe₂," *Opt. Express* **26**(17), 21501–21509 (2018).
- 40. Q. Cui et al., "Transient absorption measurements on anisotropic monolayer ReS₂," *Small* **11**(41), 5565–5571 (2015).

Biographies of the authors are not available.